2022 EAGE ANNUAL
83RD CONFERENCE & EXHIBITION
MADRID I SPAIN

DEPTH IMAGING IN NORTH KUWAIT: CHALLENGES AND SOLUTIONS

T. Rebert[1], L. Vivin[1], O. Bouhdiche[1], C. Bossy[1], F. Haouam[1], N. Rordjaroenpan[1], M. Retailleau[1], D. Le Meur[1], A. El-Emam[2], M. Ali[2], H. Bayri[2]

[1] CGG; [2] Kuwait Oil Company (KOC)

Summary

We present the main results of a tailored velocity model building workflow on a recent broadband survey from North Kuwait. Depth imaging in Kuwait presents several challenges, including the need to capture the strong velocity variations of a complex near surface that generates long and short wavelength distortions, the need for a detailed velocity model to accurately restore the structures of low-relief and faulted Cretaceous and Jurassic traps, and the difficult imaging of the Paleozoic structure hidden below a curtain of multiples. First, we give insight on a Multi-Wave Inversion and Full-Waveform Inversion workflow, which exploited the finely sampled surface waves and the diving waves to derive a high-resolution near-surface P-wave velocity model. Then we show how high-definition Multi-Layer Tomography is able to capture the complex velocity variations within the Cretaceous, which helps resolve imaging distortions. Finally, we focus on the imaging of the Paleozoic structures, which are key to understanding the regional geological history.

Depth imaging in North Kuwait: Challenges and solutions

Introduction

Depth imaging in North Kuwait presents several challenges that we endeavoured to solve through a high-end velocity model building workflow. We will present the main results of our tailored velocity model workflow on a recent broadband survey from North Kuwait. First, we will show how the complex near-surface, which generates strong distortions on the time image, was characterized through Multi-Wave Inversion, reflection/refraction tomography and Full-Waveform Inversion. Then, we will show how high-definition, well-constrained tomography was able to capture the short- and long-wavelength velocity variations within the Cretaceous and Jurassic. Finally, we will focus on the imaging of the Paleozoic structures, which are key to understanding the regional geological history.

Context

The dataset in this case study stemmed from two broadband, single-source, single-sensor, wide-azimuth surveys from North Kuwait, acquired in 2012 and 2016 respectively. They were acquired with a dense 25 m shot and receiver point interval, with each receiver line consisting of four (survey 1) or two (survey 2) sub-lines of point receivers arranged in a staggered pattern (El-Emam and El-Saaba, 2015). The two surveys were merged during the pre-processing of the datasets, totalling an imaging area of 2500 km^2. The pre-processing included advanced surface-wave and guided-wave modelling and attenuation, surface-consistent processing for static corrections and deconvolution, which resulted in stable, broadband signal content, and modelling/subtraction of surface multiples and main internal multiples whose generators were identified on VSPs. Finally, the data were regularized through anti-leakage 5D interpolation.

Near-surface P-waves velocity characterization

A near-surface velocity field is usually characterized using refraction tomography of the P-wave first breaks. This technique yields velocity models with good spatial resolution but often lacks vertical resolution and does not allow capture of shallow velocity inversions. To address this challenge, we used Multi-Wave Inversion (MWI), which exploits the surface waves and interpreted shallow two-way time horizons, in addition to the diving waves (Bardainne, 2018). The 12.5 m receiver interval enabled reliable Dispersion Curve picks up to 12 Hz.

On this survey, the clear separation between hard and soft near-surface conditions, which vary with the nature of the consolidated shallow sandstones, can be identified on first break arrival times (Fig 1a) and on the 9 Hz ground-roll phase velocity (Fig 1b). The third ingredient to the joint inversion was a shallow two-way-time horizon interpreted on the near-surface image built from surface-consistent deconvolution operators (Retailleau, 2015). This image (Fig 1c) does not suffer from low signal-to-noise ratio and irregular offset distribution, unlike the image built from primary reflections in a standard survey (Fig 1d).

The initial P velocity model was a Dix-converted pre-stack time migration velocity field. The MWI result well captured the boundary between the higher near-surface velocities in the North and the lower ones in the South, achieving a higher vertical and spatial resolution with sharper shallow channels in the South-East part of the analysed zone (Fig 2c). Moreover, the long- and mid-wavelength distortions were reduced in the image (Fig 2d). The well-to-seismic ties on the Dammam and Rus horizons were considerably improved to a residual mis-tie of 2 m. After analysing the maximum penetration depth of the surface waves and diving waves, the MWI result is only considered down to an estimated 200-250 m below the surface.

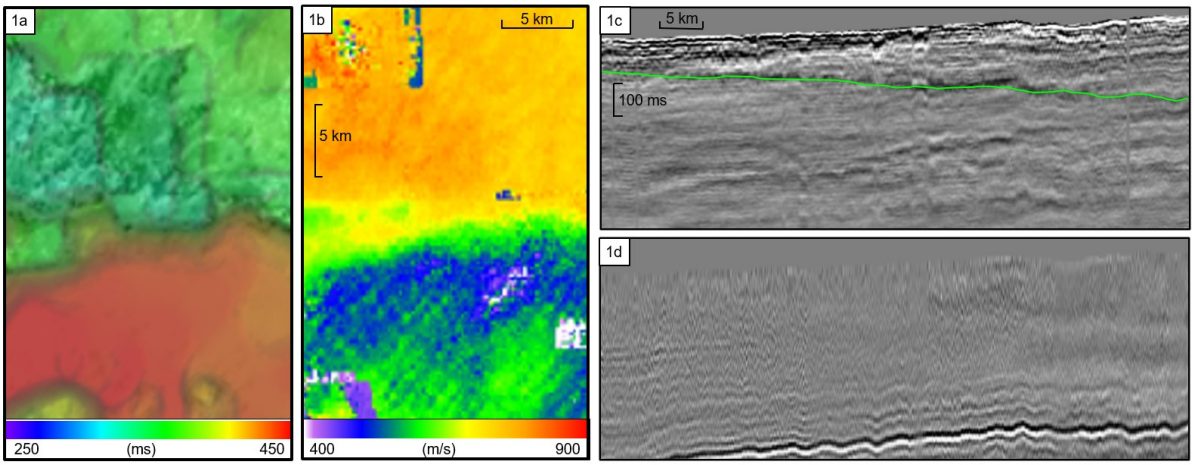

***Figure 1**: Input data for MWI: First break map for an offset of 600 m (1a), Phase velocity map at 9 Hz (1b), Shallow horizons in the first 100 ms below the surface can be more easily picked on deconvolution operators (1c) than on the recorded seismic where they are difficult to interpret (1d). The horizon used for MWI is overlaid on deconvolution operators on Fig 1c.*

Joint Refraction-Reflection tomography and Full Waveform Inversion

The updated P-wave velocity from MWI was integrated into the initial depth P-wave velocity model for joint reflection/refraction tomography (Allemand et al., 2017), which used full-azimuth, de-migrated Common Incidence Gather (CIG) picks and the first breaks to update the shallow P-wave velocity and anisotropy models between the base Dammam and Rus horizons. Then, the velocity and anisotropy model were used as a starting model for anisotropic Full-Waveform Inversion (FWI). Optimal Transport FWI (OT-FWI) was used for the updates in this study as it is less prone to data mismatch than the classical least-squares approach. For OT-FWI, the cost functions are based on p-Wasserstein distances, which are multi-dimensional in data space and insensitive to random noise but sensitive to global trace-shifts (Poncet et al., 2018). Topographical effects were handled with the approach proposed by Royle et al. (2020). The FWI was run up to a maximum frequency of 12 Hz. As shown in Fig 2, the resulting velocity model yielded more coherent and simpler structures while further reducing the well mis-ties.

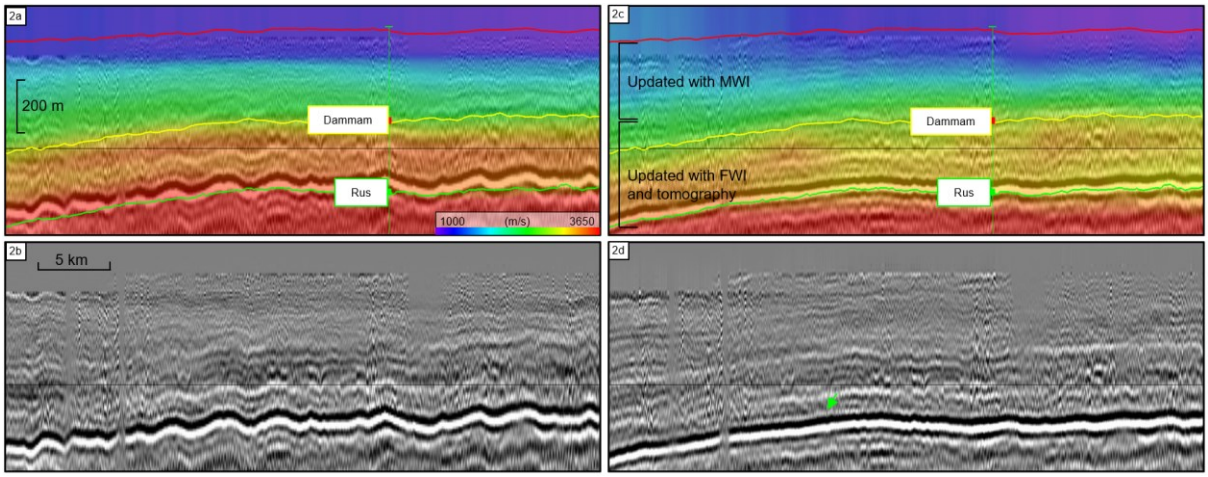

***Figure 2**: Velocity model and seismic section before near-surface model update (2a and 2b) and after (2c and 2d). Distortions at the Rus horizon (shown by green arrow) are clearly reduced, indicating that velocity anomalies above it are captured more accurately.*

Cretaceous and Jurassic well-constrained tomographic update

The near-surface model was merged below the Rus with the Dix-converted pre-stack time migration velocity field and used to migrate the regularized data to a dense set of multi-azimuth CIGs. The Cretaceous was still affected by significant distortions, which could only be generated by velocity heterogeneities located below the Rus. This was also causing amplitude dimming of deeper Jurassic horizons. In order to solve these distortions, we implemented two passes of multi-layer tilted transverse isotropic non-linear slope tomography (Guillaume et al., 2012) on the multi-azimuth CIGs. The advantage of multi-layer tomography is its ability to perform a global update of several layers simultaneously while updating the layer boundaries fitting the well markers.

Fig 3 shows the high-frequency updates yielded by the multi-layer tomography, which helped resolve short-wavelength distortions observed on the seismic image. The well tie constraint ensured that longer wavelength changes in the Jurassic were consistent with the observed structures. The average mis-tie at Jurassic targets was reduced to less than 5 m.

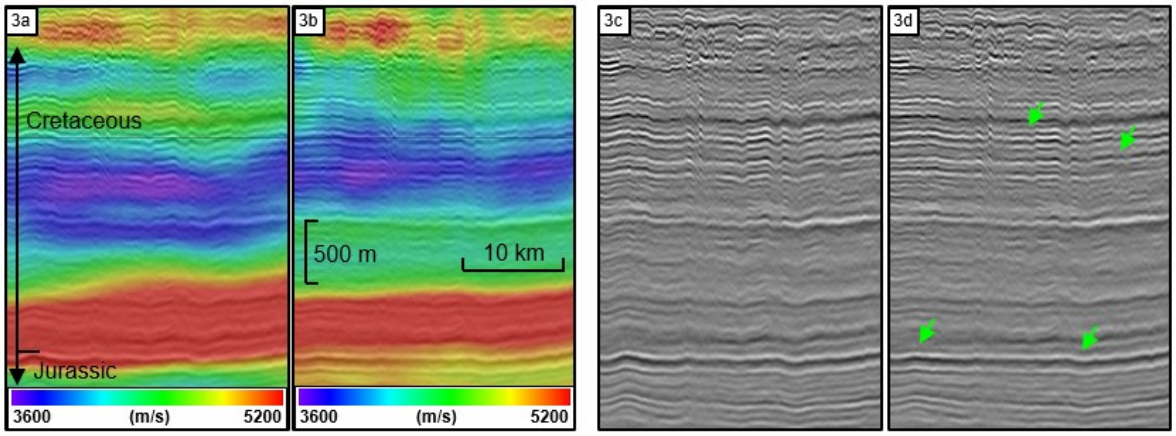

***Figure 3**: Seismic section overlaid with the velocity model before (3a) and after (3b) the second pass of high-resolution tomographic update. (3c) and (3d) show corresponding seismic sections. Green arrows indicate where distortions due to high-velocity contrasts in the Cretaceous layers are reduced. It improves focusing of the main events and increases confidence in the interpreted structures.*

Paleozoic velocity update through targeted demultiple and RTM scans

The last step of our depth imaging workflow was the update of the Paleozoic interval. The main challenge was to reveal the primary information hidden behind a curtain of multiples generated by strong Permian and Mesozoic reflectors above the unconformity. We took advantage of the structural dip discrimination between the flattish multiples and the tilted and folded Paleozoic layers underneath to produce clear images (see Fig 4). The data after demultiple allowed us to pick the main geological boundaries and to assess different velocity model scenarios (e.g., constant velocities, gradient) through Reverse Time Migration (RTM).

Conclusions

We demonstrated how we overcame depth imaging challenges in North Kuwait through a tailored velocity model building workflow. The near-surface characterization using MWI, joint reflection/refraction tomography and FWI and the well-constrained tomography update of the Cretaceous and Jurassic helped reduce imaging distortions visible from the near-surface to base Jurassic and yielded better event focusing. The Paleozoic structures were revealed thanks to an effective demultiple and a targeted velocity update using RTM scans. The final depth volume showed good ties between horizon depths and well markers.

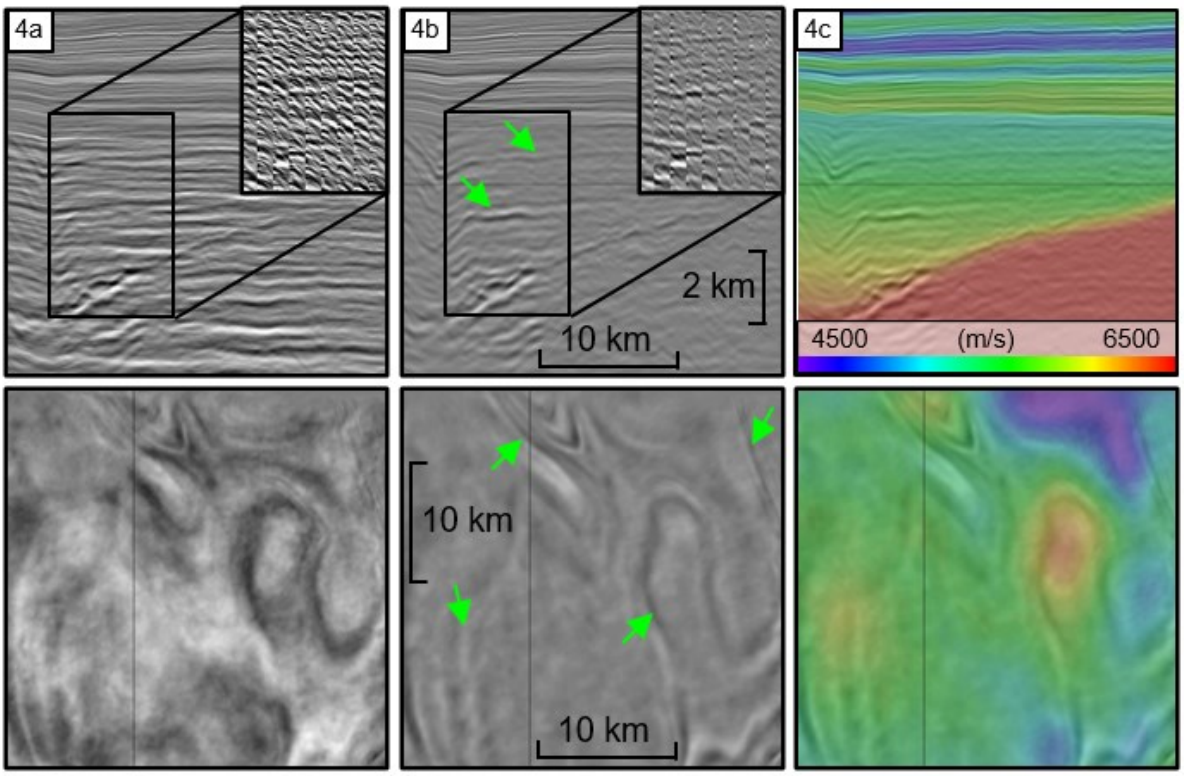

***Figure 4**: Seismic section of the Paleozoic layers, before demultiple and deep update (4a), after demultiple and deep update (4b). (4c) shows the velocity model overlaid on the seismic. On the top row, a vertical section is displayed; on the bottom row, a depth slice is displayed. The demultiple reveals primaries hidden below the curtain of multiples (green arrows) and helps build a geological model. Common Image Gathers are also displayed on the top right-hand corner of (4a) and (4b) showing the amount of multiples removed and the flat primaries behind the strong multiples.*

Acknowledgments

We are grateful to the Kuwait Oil Company & CGG for their permission to publish this study. We also thank all those who were involved in the project.

References

Allemand, T., Sedova, A. and Hermant, O. [2017] Flattening common image gathers after waveform inversion: the challenge of anisotropy estimation. *88th SEG International Meeting*, Expanded Abstracts, 1410-1415.

Bardainne, T. [2018] Joint inversion of refracted P-waves, surface waves and reflectivity. *80th EAGE Conference & Exhibition*, Extended Abstracts, We K 02.

El-Emam, A.H. and El-Sabaa, A. [2015] Quantitative Analysis of Point Receiver 3D Seismic for Optimum and Cost Effective Survey Design, Case Study. *77th EAGE Conference & Exhibition*, Extended Abstracts, Th P7 08.

Guillaume, P., Hollingworth, S., Zhang, X., Prescott, A., Jupp, R. and Pape, O. [2012] Multi-layer tomography and its application for improved depth imaging. *82nd SEG International Meeting*, Expanded Abstracts.

Retailleau, M.G. [2015] Imaging the Near Surface Using Surface-consistent Prediction Operators - Examples from the Middle East. *77th EAGE Conference & Exhibition*, Extended Abstracts, Th N116 09.

Royle, G, Leblanc, O., Viguier, G., Lambaré, G., Sedova, A., Shutova, S. and Carotti, D. [2020] Acoustic Land Full-Waveform Inversion with Free-Surface Topography in Oman. *82nd EAGE Conference & Exhibition*, Extended Abstracts.